ISBN: 978-3-95450-227-1 ISSN: 2673-5490 doi:10.18429/JACoW-IPAC2022-MOPOTK046

DESIGN CONCEPT FOR A SECOND INTERACTION REGION FOR THE ELECTRON-ION COLLIDER*

B.R. Gamage†, V. Burkert, A.K. Draees, R. Ent, Y. Furletova, D. Higinbotham, T. Michalski, R. Rajput-Ghoshal, D. Romanov, T. Satogata, A. Seryi, A. Sy, C. Weiss, W. Wittmer, Y. Zhang, Jefferson Lab, Newport News, VA, USA
E.-C. Aschenauer, J.S. Berg, A. Jentsch, A. Kiselev, C. Montag, R. Palmer, B. Parker, V. Ptitsyn, F. Willeke, H. Witte, Brookhaven National Lab, Upton, NY, USA
V.S. Morozov, F. Lin, Oak Ridge National Lab, Oak Ridge, TN, USA
C.E. Hyde, Old Dominion University, Norfolk, VA, USA
P. Nadel-Turonski, Stony Brook University, Stony Brook, NY, USA

Abstract

In addition to the day-one primary Interaction Region (IR), the design of the Electron Ion Collider (EIC) must support operation of a 2nd IR potentially added later [1, 2]. The 2nd IR is envisioned in an existing experimental hall at RHIC IP8, compatible with the same beam energy combinations as the 1st IR over the full center of mass energy range of ~20 GeV to ~140 GeV. The 2nd IR is designed to be complementary to the 1st IR. In particular, a secondary focus is added in the forward ion direction of the 2nd IR hadron beamline to optimize its capability in detecting particles with magnetic rigidities close to those of the ion beam. We provide the current design status of the 2nd IR in terms of parameters, magnet layout and beam dynamics.

INTRODUCTION

A preconceptual design of the second IR must satisfy the physics requirements with magnets consistent with NbTi superconducting magnet technology, and with a footprint fitting in the RHIC IP8 experimental hall along with other beam lines. Here we focus on the design of the hadron beamline since it includes a special feature of the secondary focus for detection of particles with low transverse momentum and near or above the beam magnetic rigidity. The design is constantly evolving to better accommodate the secondary focus along with the required accelerator components necessary to accommodate the detector [3]. The current layout of the EIC is shown in Fig. 1. The IRs are specified by their locations in the tunnel with the primary IR being at IP6 and second IR being at IP8. Table 1 shows a comparison of some of the critical parameters of the two IRs. Some of the key design differences of the IR8 from the IR6 are the addition of a second focus and a larger crossing angle.

Crossing Angle

One of the geometrical differences between IR8 and IR6 is that the hadron beam crosses the electron beam going from the outer to the inner wall of the tunnel [4]. The interaction point (IP) is moved radially inwards from the hall center toward the center of the ring to accommodate the RCS bypass (as shown in Fig. 1). This shortens the distance before the downstream hadron beamline reaches the inner wall of the experimental hall. A large crossing angle such as 50 mrad is undesirable mainly due to the hall geometry and the issues arising due to the crab cavities. The beta functions at the crab locations are optimized to reduce the required crabbing voltage while keeping the beam size consistent with the crab cavity aperture limit. Any increase in the crossing angle would require additional crab cavities, straining the space requirements. Extra crab cavities would also introduce more impedance and cause other dynamical issues.

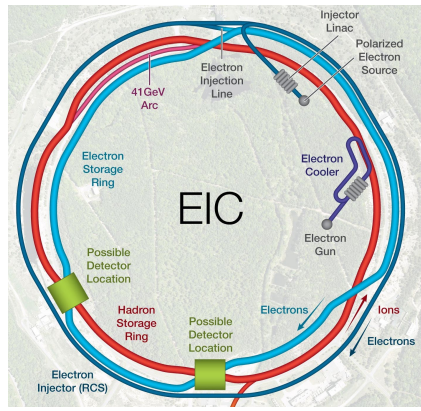

Figure 1: Layout of the EIC complex indicating the hadron storage ring (HSR), electron storage ring (ESR) and rapid cycling synchrotron (RCS). The primary IR is located at the 6 o'clock position while the second IR is located in the 8 o'clock position.

A lower crossing angle such as 25 mrad as in IR6 is more favorable from this point of view. However, the beam crossing configuration and the hall geometry prevent one from bending hadrons away from electrons as in IR6. For this reason, a larger crossing angle is needed to accommodate the hadron and electron magnets and keep the magnetic cross-talk between them at an acceptable level. This also results in placement of the zero degree calorimeter (ZDC) in IR8 on the inside of both beam lines as opposed to between

* This material is based upon work supported by Jefferson Science Associates, LLC under Contract No. DE-AC05-06OR23177, Brookhaven Science Associates, LLC under Contract No. DE-SC0012704 and UT-Battelle, LLC, under contract No. DE-AC05-00OR22725 with the U.S. Department of Energy.
† randika@jlab.org

ISBN: 978-3-95450-227-1 ISSN: 2673-5490 doi:10.18429/JACoW-IPAC2022-MOPOTK046

Table 1: Summary of the 2nd IR Design Requirements and their Comparison to the 1st IR

Parameter	EIC IR 6	EIC IR 8	Impact
Crossing angle [mrad]	25	35	p_T resolution, acceptance, geometry.
Detector space symmetry [m]	-4.5/+5	-4.5/+5	Forward/rear acceptance balance.
Forward angular acceptance [mrad]	20	25	Spectrometer dipole aperture.
Far-forward angular acceptance [mrad]	4.5,4.5	5,4.5	Neuton cone, p_T^{max}.
Minimum $\Delta(B\rho)/(B\rho)$ allowing for detection of $p_T = 0$ fragments	0.1	0.003-0.01	Beam focus with dispersion, reach in x_L and p_T resolution, reach in x_B for exclusive process.
Angular beam divergence at IP, h/v,rms [mrad]	0.1/0.2 adjustable	0.1/0.2 adjustable	p_T^{min}, p_T resolution.
Low Q^2 electron acceptance	< 0.1	< 0.1	Not a hard requirement.

the beam lines as in IR6. Following the above reasoning, a crossing angle of 35 mrad was chosen for IP8.

Second Focus

Two key parameters used to measure the acceptance of a scattered particle are x_L, which is the fraction of the longitudinal momentum relative to the nominal momentum of the hadron beam, and p_T, which is the fragment's transverse momentum component (or $p_T \simeq \theta p$ where p is the particle momentum). In exclusive high-energy scattering processes on the proton or on nuclei, the fractional longitudinal loss of the beam is equal to the Bjorken scaling variable$1 - x_L \simeq x_B$; the acceptance in x_L therefore directly determines the physics coverage in x_B for such measurements [5]. A scattered particle that escapes the main detector and the forward spectrometer dipole, $B0$, can still be detected if its x_L does not exceed a maximum value to first order given by

$$x_L < 1 - 10\frac{\sqrt{\beta_x^{2nd}\epsilon_x + D_x^2\sigma_\delta^2}}{D_x}, \quad (1)$$

where β_x^{2nd} is the horizontal Twiss β-function at the 2nd focus, ϵ_x is the horizontal beam emittance, D_x is the horizontal dispersion and σ_δ is the beam rms momentum spread. By having a second focus with a low beta function β_x^{2nd} and a high dispersion D_x, one can closely approach the fundamental limit on x_L of $x_L < 1 - 10\sigma_\delta$. For the current optics and beam parameters listed in Table 2, the limiting x_L that can be measured at the second focus is 0.9932, while the maximum detectable $x_L = 0.9928$. Further improvement is presently limited by the obtainable beam parameters, ϵ_x and σ_δ.

Table 2: Selected Optics and Beam Parameters at the Second Focus

Parameter	Value	Units
β_x	0.62	m
D_x	0.38	m
ϵ_x	11.3	nm
σ_δ	6.8×10^{-4}	-

LAYOUT AND OPTICS

The current layout of IR8 in the IP8 experimental hall is shown in Fig. 2 and optics in Fig. 3. The second focus is located at $s \simeq 47$ meters. Both the electron and hadron beamlines are matched to the corresponding collider arcs (ARC7 and ARC9) in terms of geometry and optics.

The optics and design for the IR8 electron beamline is similar to that of IR6. There are only small changes in the dipole magnets to compensate for the increase in the bending angle, the change in the direction of beam crossing and the differences in the hall geometry. There are crab cavities and a spin rotator in the hadron beam line on each side of the IP. Integration of the second focus into the forward side leaves space of only $\simeq 50$ m for optical and geometric matching. This imposes a challenging constraint on the magnet parameters.

Acceptance Optimization

The downstream optical elements between the IP and the second focus including the four final focusing quads and the two dipole correctors must have sufficiently large apertures to provide clear passage for scattered particles up to the required p_T. Neutral particles travel in straight lines to the ZDC while charged particles with high x_L closely follow the hadron beam to the second focus where two Roman pots are placed. The limit on the maximum magnetic field attainable with the NbTi superconducting magnet technology and the quadrupole field gradients required for appropriate beam focusing at the IP set limits on the quadrupole aperture size. Not only the configuration, lengths and strengths of these magnets but their orientations(rotation about the vertical axis and transverse shift) have been optimized to provide the maximum acceptance coverage to both neutral and charge scattered particle types. Figure 4 illustrates the optimized forward acceptance to charged particles with $p_0 \simeq 275$ GeV and neutral particles. The second IR acceptance is optimized for the highest proton beam energy of 275 GeV. Similar acceptance performance is expected at lower energies.

ONGOING WORK

Simultaneous operation of two detectors in the EIC is currently envisioned using two equal bunch trains with all

ISBN: 978-3-95450-227-1 ISSN: 2673-5490 doi:10.18429/JACoW-IPAC2022-MOPOTK046

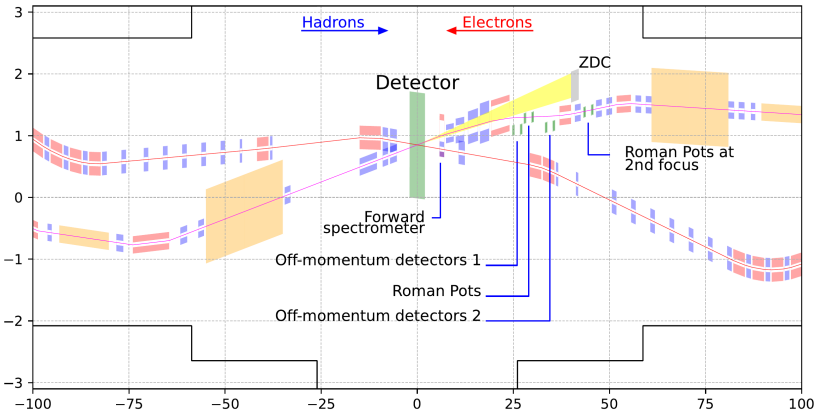

Figure 2: Layout of the second IR with a 35 mrad crossing angle indicating locations of the main forward and auxiliary detector components. The black solid lines outline the size of the IP8 experimental hall and adjacent tunnel. Pink and purple represent dipole and quadrupole magnets, respectively. The detector solenoid is shown in green at the center. Orange is for special accelerator equipment such as crab cavities and hadron spin rotators. The yellow shaded area indicates a ±5 mrad cone of neutral particles traveling towards the ZDC. Space is available for luminosity monitor, low Q^2 tagger and local hadron polarimeter (not shown).

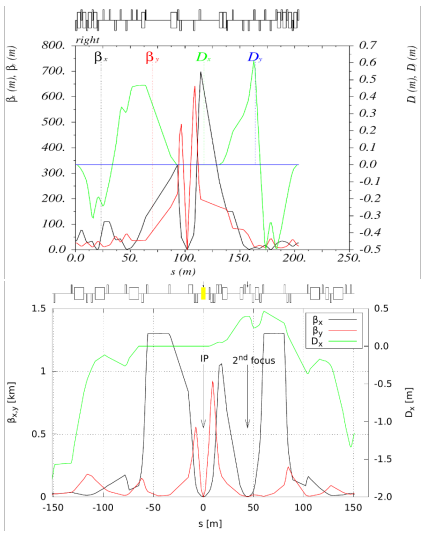

Figure 3: Optics of the 10 GeV electron (top) and 275 GeV proton (bottom) IR8 beam lines. The horizontal and vertical β functions (left vertical scale) and the horizontal dispersion D_x (right vertical scale) are plotted versus the distance along the beam s.

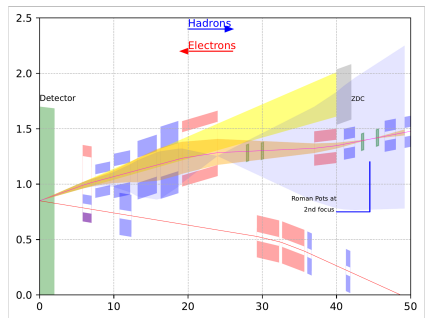

Figure 4: Forward side of IR8 illustrating acceptance to protons and neutrons. Yellow shows neutral particles within a ±5 mrad cone, orange is for protons with $x_L = 1 (\Delta p/p = 0)$ and $p_T \leq 1.37$ GeV and blue is for protons at $x_L = 0.5 (\Delta p/p = 0.5)$ and $p_T \leq 0.69$ GeV

.

bunches in the first train colliding only at IP6 and all bunches in the second train colliding only at IP8 [6]. Such an operation requires the IP of the 2nd IR to be shifted longitudinally to prevent collisions of the same bunch at both IPs. Design changed are underway to accommodate this shift by moving IP8 clockwise away from IP6.

Engineering feasibility of the large-aperture high-gradient IR8 magnets is being evaluated. The IR8 design is being optimized to ensure that the IR8 magnets are operating at the same engineering constraints as the IR6 ones. In particular, the required magnet field quality is one of the parameters that is being studied. Every effort is being made to reuse existing RHIC magnets as much as possible. The need for new magnets to improve the IR8 performance is also being considered. It is assumed that any new magnets would still be consistent with the NbTi technology but would go up to higher fields than the existing RHIC magnets.

SUMMARY

The conceptual design of the second IR has made significant progress over the recent months. The detection requirements are satisfied while considering the spacial, dynamical, and engineering constraints in a consistent way. The IR8 design take full advantage of the knowledge and experience gained from the IR6 design. Optimization, refinement and updates are in progress to further optimize IR8 performance and accommodate modification requests originating from optimization and work on self-consistency of the entire EIC complex.

ISBN: 978-3-95450-227-1 ISSN: 2673-5490 doi:10.18429/JACoW-IPAC2022-MOPOTK046

REFERENCES

[1] A. Aprahamian *et al.*, "Reaching for the horizon: The 2015 long range plan for nuclear science", *DOE/NSF Nuclear Science Advisory Panel (NSAC) Report*, Okt. 2015.

[2] "An Assessment of U.S.-Based Electron-Ion Collider Science", Washington DC, 2018. doi:10.17226/25171

[3] B. R. Gamage *et al.*, "Design Concept for the Second Interaction Region for Electron-Ion Collider", in *Proc. IPAC'21*, Campinas, Brazil, May 2021, pp. 1435–1438. doi:10.18429/JACoW-IPAC2021-TUPAB040

[4] C. Liu *et al.*, "Reconfiguration of RHIC Straight Sections for the EIC", presented at the IPAC'22, Bangkok, Thailand, Jun. 2022, paper WEPOPT034, this conference.

[5] R. Abdul Khalek *et al.*, "Science Requirements and Detector Concepts for the Electron-Ion Collider: EIC Yellow Report", 2021. doi:10.48550/arXiv.2103.05419

[6] J. Beebe-Wang *et al.*, " Electron Ion Collider Conceptual Design Report", 2021. doi:10.2172/1765663